How stable are amphiphilic dendrimers at the liquid/liquid interface?

D. L. Cheung [a,*], P. Carbone [b]

[a] Department of Chemistry and Centre for Scientific Computing, University of Warwick, Coventry, CV4 7AL, UK.

[b] School of Chemical Engineering and Analytical Science, The University of Manchester, Manchester, Oxford Road, M13 9PL, UK

Abstract

By means of molecular dynamics simulations the free energy of adsorption of model dendrimer characterized by monomers of different chemical affinity is predicted as a function of the number and position of the monomers. The results show that modifying the affinity of the only end-monomers with one of the two solvent components (amphiphilic dendrimer) is enough to remarkably increase the stability of the molecule at the interface. The results also indicate that the the so called Janus-dendrimer, where only half of the end-monomers are modified, does not show a higher interfacial stability compared with standard amphiphilic one. These findings compare well with simulation results obtained from atomistic simulations performed on polyaminoamide dendrimer at the air/water interface. The free energy profiles have also been compared with those obtained from simpler models which treat the dendrimer molecule as a hard sphere showing that such simplification is acceptable in poor solvent but not in good solvent where the flexibility of the dendrimer molecule plays a major role in its stability at the interface. These calculations will help in the design of new amphiphilic dendrimers and in predicting their properties at liquid/liquid interface.

Corresponding authors:
Email: david.cheung@warwick.ac.uk
Email: paola.carbone@manchester.ac.uk
***Present address: Department of Physics and Centre for Scientific Computing, University of Warwick, Coventry, CV4 7AL, UK**

Introduction

Dendrimers are a class of macromolecules characterized by a high degree of symmetry in their structure[1] and since their discovery they have been increasingly employed for different applications such as drug and gene delivery or ultra sensitive sensors[2, 3]. Dendrimers show in fact structural properties both in bulk, solution and interface that are unique to them. In particular, the possibility of decorating their terminal monomers with a different variety of chemical functions makes dendrimers interesting building blocks for a large range of interfacial materials.[4] Due to the large number of functionalized end groups and their symmetric topology, dendrimers can in fact bind tightly at the interface allowing the formation in water of a large variety of self assembled structures that can be exploited for several applications such as encapsulation or delivery of drugs. [5-11] The synthesis of such multi-function compounds where several chemical functions are combined in one single molecule, is however not trivial. Experimentally several synthetic routes have been proposed to functionalise dendrimers with different chemical groups and some of them allow even the selective functionalization of only one side to the molecule. [12, 13] These latter types of synthetic procedures allow the preparation of amphiphilic "Janus" dendrimers, where the specific chemical blocks are attached only to part of the end-monomers breaking the symmetry of the macromolecule.[13] However, due to the difficulties encountered in their synthesis, there are a relatively limited number of examples of Janus dendrimers when compared to the symmetrical ones. In order to guide the synthesis of these materials, it would be therefore ideal to have a simple model or a theoretical approach able to predict the dendrimers interfacial properties as a function of the polarity and/or reactivity and position within the dendrimer molecule of the grafted chemical functions.

While the behaviour of molecules at liquid interfaces has been long studied theoretically both using analytic and semi-analytic theories, where their adhesion to liquid interfaces is interpreted as a result of the molecule (generally identified as a solid particle) wettability and changes in interfacial area,[14, 15]computer simulations are ideally suited to study the mechanism of adsorption of molecules on liquid interfaces.[16] Using molecular simulations it has been shown that macroscopic treatments can accurately predict adsorption strengths for particles as small as ~5nm, however, studies have revealed that macroscopic theories can fail in predicting the strength of interactions for smaller particles and the range of the nanoparticle/interface interactions. [17-20] For example, monitoring the free energy profile of nanoparticles at liquid interfaces, simulations have shown that the interaction between the nanoparticle and the interface (for rigid uniform spherical nanoparticles) was both longer ranged and softer than predicted by theory[17, 18]due to broadening of the interface by capillary

waves. [21] Simulations have been also performed on rigid Janus (amphiphilic) nanoparticles showing that the fact each hemisphere favourably interacts with one of the two fluids increases the stability of the particle at the interface. Besides the simplified models mentioned above, where the molecule at the interface is described as a single hard sphere, more detailed molecular models have been also used. For example using atomistic molecular dynamics simulations Tay and Bresme predicted the contact angle, particle shape and orientational order of the water molecules for one alkylthiolpassivated gold nanoparticle adsorbed on the air-water interface. [22] More recently an atomistic model has also been used to simulate amphiphilic dendrimer at the air/water interface.[23] The simulations have showed that the flexible polyaminoamide (PAMAM) dendrimers functionalized with long aliphatic chains adhere to the air/water interface adapting their molecular conformation to the polar/apolar environment. The atomistic simulations have also demonstrated that the geometrical orientation of the molecule follows that predicted by the analytical models and that most of the dendrimer conformation changes are driven by the formation and breakage of hydrogen bonds between the dendrimer amide groups and the water molecules. The simulation results have also indicated that, at least neglecting dendrimer-dendrimer interactions (i.e. at very low concentration of dendrimer), fully functionalized and Janus dendrimers (i.e. dendrimers where either all or only half of the end-monomers are functionalized) show a similar interfacial stability suggesting that maybe the effort required to synthetize asymmetric dendrimer molecules might not be necessary if only interfacial stability is sought.

Although atomistic models enable to monitor in great details all the chemical interactions between the particle and the interfaces, the computational cost of such simulations performed on macromolecules at liquid/liquid interface is high. Being available in the literature both the results of extremely simplified models [20] and very detailed ones, [23] we can now verify whether models retaining only the characteristic topology of dendrimer molecules but not their chemical specificities can properly describe the behaviour of these molecules at the liquid/liquid interfaces.

The aim of this paper is therefore to study the stability of model dendrimers at fluid/fluid interface modifying the affinity of their monomers for one of the two liquids as a function of monomer position in the dendrimer structure. By calculating the free energy profile associated to the detachment of the dendrimer from the interface, the relative stability of Janus and symmetrically functionalized dendrimers can be compared and the effect of the structural parameters, such as the intrinsic rigidity of the dendrimer structure, on the stability of the molecule at the interface can be identified. Finally the results obtained from the free energy calculations can be compared with those obtained from macroscopic theories and simulations performed on hard sphere and on all-atom model of dendrimers.

Simulation and model details

In this study we consider dendrimers of identical topology (d2g3) corresponding to a third generation (g3) dendrimer with each branching bead having a connectivity of two (d2) (illustrated in Figure 1).[24] In the Figure 1 beads with different connectivity and position in the dendrimer structure are named differently: the end-dendron beads with one covalent bond are named E1 and E2 (coloured blue or yellow in Figure 1) while the internal beads, named I and coloured black in Figure 1, include the linear separator beads with two covalent bonds and the branching beads with three covalent bonds. During the simulation a single d2g3 dendrimer sis placed at the liquid/liquid interface and the strength of the interactions between the dendrimer beads and the two solvent components (denoted S1 and S2) is varied. 24000 solvent beads were considered, with S1 beads initially placed in the region $z<0$ and S2 beads in $z>0$. In order to examine the relationship between dendrimer stability and its functionalization three distinct dendrimer models, uniform, Janus (amphiphilic), and core shell, are investigated. For the uniform dendrimer the interactions between all the dendrimer and solvent beads are identical, either repulsive or attractive (poor and good solvent respectively). For the Janus dendrimer the interactions between the internal (I) beads have repulsive interactions with both solvent components, while the two different types of end beads, E1 and E2, have attractive interactions with opposite solvent components S1 and S2 respectively. In order to examine the effect of the placement of the different end groups on the stability of the molecule at the interface, three different configurations of the Janus dendrimer as studied. In the first E1 and E2 beads are segregated onto different dendrons (note that as there are three dendrons in order to have an equal number of E1 and E2 end groups (selective for S1 and S2 solvent components respectively) one dendron contains both types of end groups),in the second the E1 and E2 beads alternate, and finally in the third Janus model E1 and E2 beads are randomly distributed on the dendrimer exterior (in order to sample over different dendrimer conformations, simulations were performed on five different random dendrimers). These are illustrated schematically in Figure 1.For the core-shell dendrimer the interaction between the I and E beads have attractive interactions with opposite solvent components (i.e. I beads interact favourably with S1 and unfavourably with S2, while the E beads are characterized by the opposite affinity.

The solvent is modelled as a two-component fluid, interacting through a cut and shifted Lennard-Jones potential, V_s,

$$V_S(r) = \begin{cases} 4\varepsilon\left[\left(\frac{\sigma}{r}\right)^{12} - \left(\frac{\sigma}{r}\right)^{6}\right] - V_{cut}, & r \le r_{cut} \\ 0, & r > r_{cut} \end{cases} \qquad \text{(eq. 1)}$$

where $V_{cut} = 4\varepsilon\left[\left(\frac{\sigma}{r_{cut}}\right)^{12} - \left(\frac{\sigma}{r_{cut}}\right)^{6}\right]$ and $r_{cut} = 2.5\sigma$ and $r_{cut} = \sqrt[6]{2}\sigma$ for interactions between like and unlike components respectively. The interactions between the beads within the dendrimer and between dendrimer and solvent beads are also described using the Lennard Jones potential; in all cases the interaction between beads in the dendrimer are truncated at $r_{cut} = \sqrt[6]{2}\sigma$. Table 1 summarizes the interactions between the different dendrimer models.

MONOMER TYPES / MODELS	I	E1	E2
Uniform (poor)	$\sqrt[6]{2}\sigma/\sqrt[6]{2}\sigma$	$\sqrt[6]{2}\sigma/\sqrt[6]{2}\sigma$	$\sqrt[6]{2}\sigma/\sqrt[6]{2}\sigma$
Uniform (good)	$2.5\sigma/2.5\sigma$	$2.5\sigma/2.5\sigma$	$2.5\sigma/2.5\sigma$
Core-shell	$2.5\sigma/\sqrt[6]{2}\sigma$	$\sqrt[6]{2}\sigma/2.5\sigma$	$\sqrt[6]{2}\sigma/2.5\sigma$
Janus	$\sqrt[6]{2}\sigma/\sqrt[6]{2}\sigma$	$2.5\sigma/\sqrt[6]{2}\sigma$	$\sqrt[6]{2}\sigma/2.5\sigma$

Table 1: Dendrimer-solvent interaction cut-offs for different dendrimer models. Values separated by slashes denote interaction cut-offs for S1 and S2 solvents respectively. The labels associated to the monomer types are explained in the text. See also Figure 1.

The topology of the dendrimer is defined through harmonic bonds

$$V_{bond} = \frac{1}{2}k_\ell(\ell - \ell_0)^2 \qquad \text{(eq. 2)}$$

where$k_\ell = 250\varepsilon\sigma^{-2}$ and $\ell_0 = \sigma$ are the force constant and equilibrium bond lengths respectively.

Following a previous work, [24] to include local rigidity in the dendrimer structure an additional bond angle potential (V_{angle}) is applied between beads connected by two covalent bonds

$$V_{angle} = k_\theta(\theta - \theta_0)^2 \qquad \text{(eq. 3)}$$

where $k_\theta = 100\varepsilon$ is the angle bending force constant and θ_0 is the equilibrium angle (with $\theta_0 = 180°$ or $\theta_0 = 120°$ for angles with a vertex on the linear separator beads with two covalent bonds and the branching beads with three covalent bonds respectively).

The free energy profile or potential of mean force is determined using umbrella sampling.[25] The nanoparticle z-coordinate is constrained at a series of points z_i using a harmonic potential

$$V_{umb} = \frac{1}{2}k(z - z_i)^2 \qquad \text{(eq. 4)}$$

where $k = 5 - 20\varepsilon\sigma^{-2}$. For each $z_i$the (biased) probability distribution $\wp_i(z)$ is determined and the final (unbiased) probability distribution $\wp(z)$is found using weighted histogram analysis [26]. For each z_i 6×10^6 MD steps (including10^6equilibration steps) were performed. Equilibrium positions and force constants for umbrella sampling are given in Tables 2 and 3. The free energy was then given by

$$F(z) = -k_B T \ln \wp(z) \qquad \text{(eq. 5)}$$

In order to estimate errors in the free energy profiles, each of these simulation runs were divided into five subruns with the full analysis performed on these separately.

z_i / σ	0	±1	±2	±3	±4	±5
k / **εσ**$^{-2}$	5	20	20	20	20	20
z_i / σ	±6	±6.5	±7	±8	±9	±10
k / **εσ**$^{-2}$	20	20	20	10	10	10

Table 2: Equilibrium positions and force constants for umbrella sampling on uniform and Janus dendrimers. See eqs 4 and 5 for the symbols.

z_i / σ	0	1	2	3	4	5	6	6.5
k / **εσ**$^{-2}$	5	20	20	20	20	20	20	20
z_i / σ	7	7.5	8	9	10	-1	-2	-3
k / **εσ**$^{-2}$	5	20	10	10	10	20	20	20
z_i / σ	-3.5	-4	-4.5	-5	-6	-7	-7.5	-8
k / **εσ**$^{-2}$	20	20	20	20	20	20	20	20
z_i / σ	-8.5	-9	-9.5	-10	-11	-12		
k / **εσ**$^{-2}$	20	10	10	10	20	10		

Table 3: Equilibrium positions and force constants for core-shell dendrimers. See eqs 4 and 5 for the symbols.

All simulations were performed using the LAMMPS simulation package [27]in the NPT ensemble, with $T^* = 1$ and $P^* = 1$. Temperature and pressure were controlled using a Nosé-Hoover thermostat and barostat[28] respectively; both the thermostat and barostat employed relaxation times of $0.5t^*$(where $t^* = \sqrt{m\sigma^2/\varepsilon}$). A timestep of $\delta t = 0.005t^*$ was used. In order to localise the interface in the centre

of the simulation cell repulsive walls were placed in the *z*-direction, with periodic boundaries in the *x* and *y* directions.

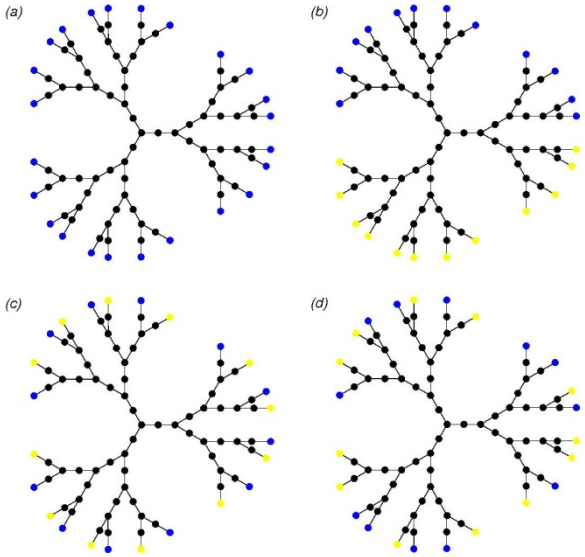

Figure 1: Schematic illustration of dendrimers studied in this work; (a) uniform/core shell dendrimer, (b) Janus dendrimer with alternating end groups, (c) Janus dendrimer with segregated end groups, and (d) Janus dendrimer with random end groups. The internal (I) beads are denoted by black circles. The end-monomer (E) beads are coloured differently (blue and yellow) in the Janus models, where they interact differently with the two solvent types, otherwise (uniform and core shell models) they are coloured only in blue.

Results

Uniform dendrimer

Shown in Figure 2 are free energy profiles for uniform dendrimer, in both poor and good solvents (note that as the interactions between the dendrimer and both solvent components are identical the free energy profiles are symmetric about z=0). In both cases the dendrimers are strongly adsorbed to the liquid-liquid interface, with desorption free energies of 100 k_BT and 75 k_BT respectively, similar in magnitude to spherical nanoparticles (both from simulation [18]and experimental [29]studies and proteins[19]).

The detachment energy for the dendrimer in good solvent is lower than in the poor solvent. In part this arises due to the attractive interactions between the dendrimer and solvent particles. When the dendrimer is at the interface it has fewer close contacts with solvent molecules, so in the good solvent case the dendrimer-solvent interaction energy increases at the interface, making this state less stable than in the poor solvent. Similar results have been seen in recent work on rigid nanoparticles.[18] In good solvent the dendrimer is also less compact than in poor solvent conditions so the effective reduction in the interfacial area is likely to be smaller (see also below).

The shape of the free energy profile, particularly in the poor solvent case, is also very similar to that found for nanoparticles; specifically the interaction is relatively long-ranged (larger than the dendrimer size), in part due to broadening of the interface by thermal capillary waves. Under poor solvent conditions the free energy increases smoothly towards before plateauing in the bulk, whereas there is some additional structure in *F(z)* in good solvent, due to changes in dendrimer configuration (see below). In neither case is an adsorption barrier seen, indicating that interfacial adsorption is purely diffusion limited, unlike recent work on nanoparticles that suggests a barrier may appear, due to electrostatic effects, rearrangement of ligands, or interface deformation.[18, 29]

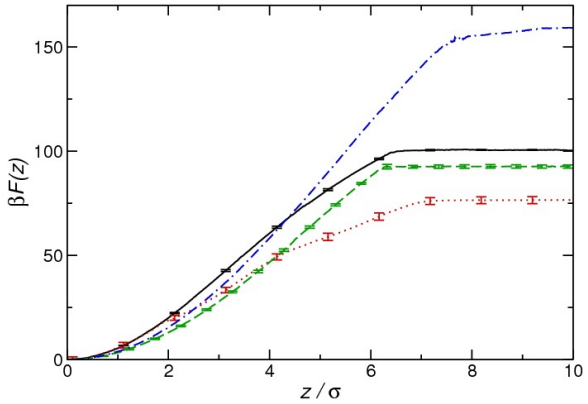

Figure 2. Free energy profile for uniform dendrimer in poor (black, solid line) and good (red, dotted line) solvents and rigid nanoparticles in poor (dashed line, green) and good (dot-dashed line, blue) solvents (details in text). *z*=0 indicates the interface.

Due to their flexibility dendrimers undergo significant conformational change when they adsorb onto interfaces and surfaces.[23] This may be seen from simulation snapshots (Figure 3(a)). When the dendrimer is in bulk solvent (z=10σ) the dendrimer is approximately spherical, whereas at the interface it assumes a disc shape (that maximises the decrease in interfacial area between the two liquid components). At intermediate distances the dendrimer elongates into an elongated shape, allowing it to contact the interface.

In order to study the effect of this conformational freedom on the interfacial stability, simulations of rigid nanoparticles of comparable size of the dendrimers were performed. The nanoparticle-solvent interaction was modelled using an expanded Lennard-Jones interaction use in previous work [18]

$$V_N(r) = \begin{cases} 4\varepsilon\left[\left(\frac{\sigma}{r-\Delta}\right)^{12} - \left(\frac{\sigma}{r-\Delta}\right)^{6}\right] - V_{cut}, r-\Delta < r_{cut} \\ 0, r-\Delta \geq r_{cut} \end{cases}$$

where $\Delta = (2R_{NP} - \sigma)/2$ (R_{NP} is the nanoparticle radius) and V_{cut} is the potential at the interaction cut-off. The nanoparticle radius was set equal to the radius of gyration of the dendrimer in bulk solution (R_{NP}=3.7 σ for poor solvent and R_{NP}=5.2 σ for good solvent) and the interaction cut-off was set to $\sqrt[6]{2}\sigma$ and 2.5σ for poor and good solvent respectively. For the poor solvent $\beta\varepsilon = 1$ (as the potential is purely repulsive the prefactor has no significant effect on anything really), while for the good solvent case $\beta\varepsilon = 2.66$, chosen to match the average dendrimer-solvent interaction energy for a dendrimer in a bulk good solvent.

For the poor solvent case the free energy profile of the rigid nanoparticle is broadly similar to that of the dendrimer (Figure 2). This similarity arises due to the collapsed nature of the dendrimer in poor solvent giving it a dense spherical structure that is similar to the rigid spherical nanoparticle. The nanoparticle is marginally less stable (~93 k_BT against 100 k_BT) and the free energy profile near z=0 is broader. These differences are attributable to changes in the dendrimer conformation in the vicinity of the interface; in particular the deformation of the dendrimer into a disk at the interface acts to increase the change in interfacial area between the S1 and S2 solvent components, leading to a larger decrease in interfacial free energy compared to the rigid case. For the good solvent case the free energy profile for the rigid nanoparticle is significantly different to the dendrimer. In this case the nanoparticle is much more stable at the interface. This difference in stability is partially explained by changes in the solvent-dendrimer (nanoparticle) interaction energy in the bulk and at the interface. Specifically when the dendrimer (in good solvent) adsorbs on the interface the interaction energy with the solvent increases by ~70 k_BT, while for the nanoparticle the increase is significantly smaller (~10 k_BT). This raised in the interfacial energy is due to the decrease in

favourable interactions with solvent particles and due to the reduced solvent density particle at the interface. As the nanoparticle is rigid this change is smaller than for the flexible dendrimer.

The change in the dendrimer shape may be quantified through the radius of gyration (R_g)

$$R_g^2 = \frac{1}{N}\sum_{i=1}^{N}(\boldsymbol{r_i} - \boldsymbol{r}_{com})^2 \qquad \text{(eq. 6)}$$

and inertia tensor ($I_{\alpha\beta}$)

$$I_{\alpha\beta} = \frac{1}{M}\sum_{i=1}^{N} m_i\left(r_i^2\delta_{\alpha\beta} - r_{i\alpha}r_{i\beta}\right) \qquad \text{(eq. 7)}$$

where $\boldsymbol{r}_i$ is the position of the *i*th monomer (relative to the dendrimer centre of mass, $\boldsymbol{r}_{com}$),m_i is the mass of the *i*th monomer,$M = \sum_{i=1}^{N} m_i$, *N* is the total number of monomers and α and β represent the three coordinate axes (x, y and z). The dendrimer axis lengths (λ_i) may be estimated from the principal moments of inertia [30]

$$\lambda_x = 2\sqrt{\frac{I_{yy}+I_{zz}-I_{xx}}{2.5M}} \qquad \text{(eq. 8)}$$

and cyclic permutations thereof. It is often convenient to order these lengths in order of size ($\lambda_{min} \leq \lambda_{mid} \leq \lambda_{max}$). The results for the uniform dendrimers are reported in Figure 3. In both poor and good solvents R_g increases at the interface, indicating the swelling of the dendrimer at the interface. There is also a secondary peak in R_g at $z\approx 5\sigma$. R_g is uniformly larger in the good solvent than in poor solvent, as may be expected. Interestingly the value of R_g in poor solvent is comparable with that obtained for dendrimer of the same generation in melt. [24] The disc-like shape of dendrimer may also be seen from the molecular axes. At the interface $\lambda_{max} = \lambda_{mid}$, indicative of disc, while as the dendrimer moves away from the interface the three axis lengths become equal before it assumes an elongated shape ($\lambda_{min} = \lambda_{mid}$).In bulk solvent (far from the interface) the three axis lengths become equal again. This progression from disc to cylinder to sphere as a function of dendrimer-interface separation is similar to that seen in atomistic simulations of PAMAM dendrimers at air-water interface [23]and for nanoparticles with grafted chains.[22, 31]

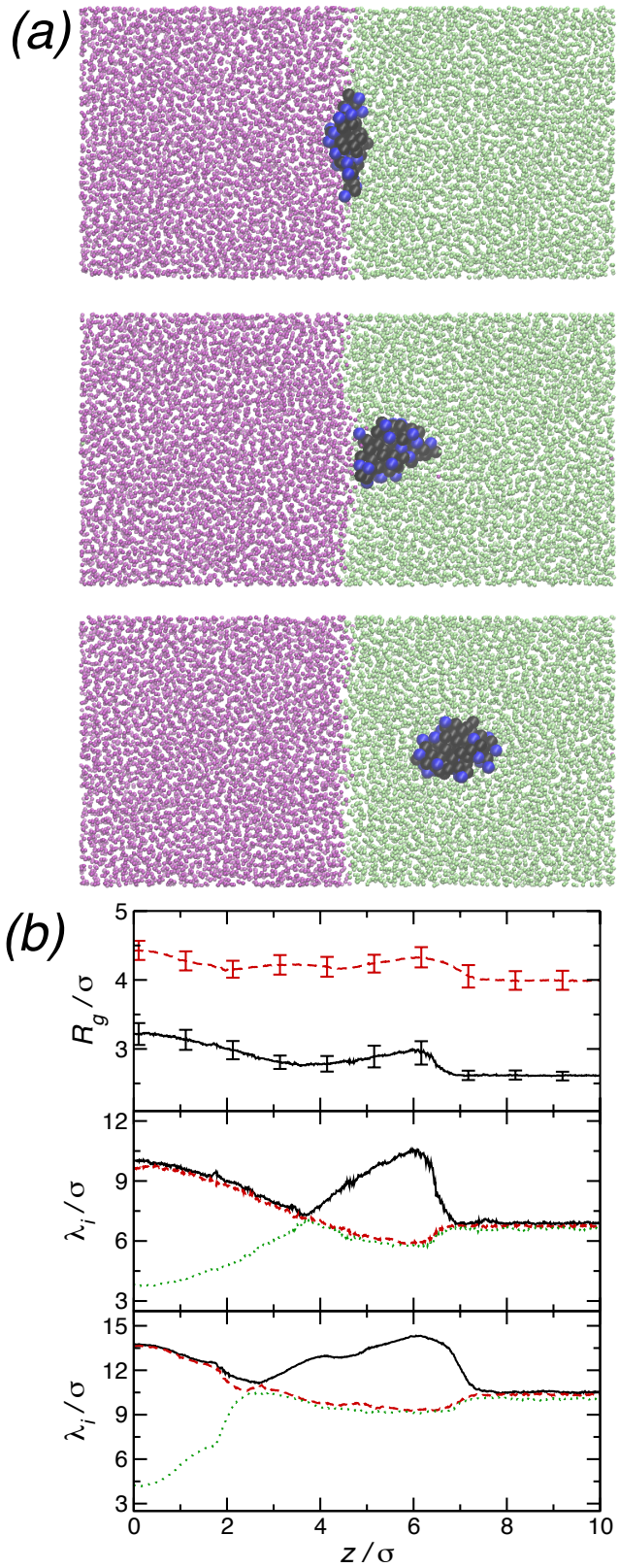

Figure 3: (a) Simulation snapshots of uniform dendrimer at liquid-liquid interface (in poor solvent), with dendrimer-interface separation z=0σ (top), z=5σ (middle), and z=10σ (bottom). Dendrimer beads coloured as in Figure 1, S1 and S2 solvent beads shown in purple and green. (b) Radius of gyration (top, red dotted line good solvent, black solid line poor solvent) and dendrimer axis lengths (from the inertia tensor eigenvalues) for uniform dendrimer in poor and good solvents(middle and bottom).

Core-Shell Dendrimers

Changing the affinity of the dendrimer beads with the solvent affects evidently the free energy profiles. The core-shell models mimic the situation in which the internal monomers (beads I) have a different chemical nature compared with the outer monomers (E) and interact favourably with opposite solvent phases.

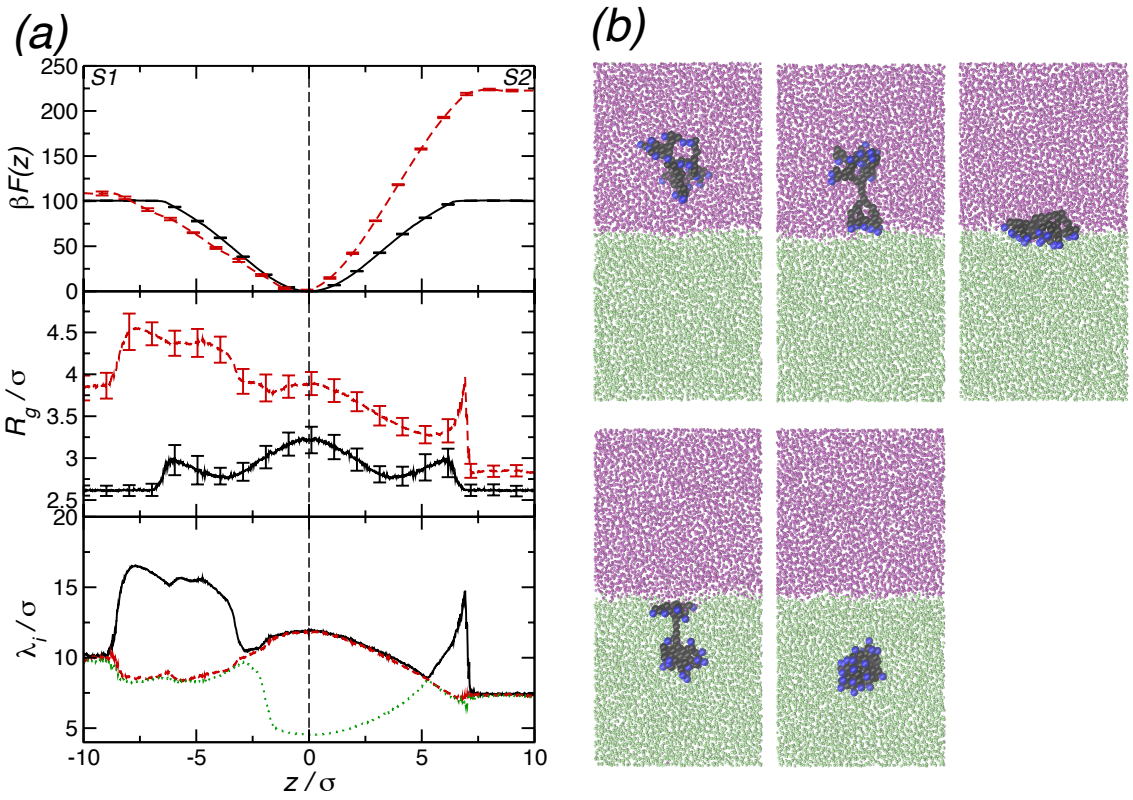

Figure 4.(a) (top) Free energy profile for uniform in poor solvent (black, solid line) and core-shell dendrimers (red, dashed line) (middle) Radii of gyration for uniform and core-shell dendrimers. (Bottom) Axis lengths ($\boldsymbol{\lambda_{max}}$ (black, solid line), $\boldsymbol{\lambda_{mid}}$ (red, dotted line), and $\boldsymbol{\lambda_{min}}$ (green, dotted line)) for core-shell dendrimer. (b) Simulation snapshots of core-shell dendrimer at liquid-liquid interface, with the dendrimer centre of mass at z=-10σ, z=-4.5σ, z=0σ, (top), z=6.5σ, and z=10σ (bottom). Beads coloured as in Figure 3(a).

Due to the introduced asymmetry within the dendrimer model, the detachment free energy profile is no longer symmetric about z=0 (Figure 4(a)). The barrier for desorption into the S1 phase (favoured solvent for the I beads) is less than half of that into S2 (favoured solvent for the E beads); this suggests that there is a considerable interaction between the dendrimer interior and the solvent and that the stability is not purely determined by the surface chemistry. The free energy of desorption into S1 is comparable with the value obtained for the uniform dendrimer in the poor solvent case. This indicates that the introduction of a relative small number of monomers that unfavourably interact with S1 (the number of end monomers is 24 out of a total of 91) in the outer part of the molecule is enough to raise the stability of the dendrimer at the interface. The dendrimer shows also a quite expanded configuration, R_g around 4.5σ (value in agreement with that obtained

for the uniform dendrimer in good solvent see Figure 3 b) as it tries to maximize the contact between the internal monomers and the solvent. The free energy of detachment into S2 is instead almost 250 k_BT, which is significantly larger than the barrier seen for the uniform dendrimer in poor solvent (where all monomers interact unfavourably with the solvent). In order to understand the origin of this large barrier it is useful to consider the change in the dendrimer-solvent interaction energies ($\Delta E_D = E_D^{Bulk} - E_D^{Interface}$) as the dendrimer adsorbs onto the interface. For the uniform dendrimer $\beta\Delta E_D = 0.32 \pm 0.03$, whereas for the core-shell dendrimer $\beta\Delta E_D = 28.4 \pm 0.1$ for entry into the S1 solvent component and $\beta\Delta E_D = 221.05 \pm 0.09$ for entry into the S2 component. This suggests that the increased stabilisation of the core-shell dendrimer is largely energetically driven and due to the high number of contacts between the different parts of the dendrimer and their favoured solvents. The compact shape (R_g less than 3σ) of the dendrimer is also a consequence of these unfavourable interactions.

The change in shape of the core-shell dendrimer is also qualitatively similar to that shown by the uniform one, with the molecule undergoing the same sphere-rod-disk transition as it approaches the interface. The shape changes are however more extreme than in the uniform case, with the core-shell dendrimer being more oblate at the interface than the uniform one. The fine structure of the core-shell dendrimer near the interface is also more complex than the uniform case (Figure 4 (b)). In particular in the intermediate region the portion of the dendrimer in contact with the interface spreads out (forming a tree or mushroom like shape), maximising the decrease in the S1-S2 interfacial area and increasing the stability of the dendrimer near the interface.

'Janus' dendrimers

As well as differences between the dendrimer interior and exterior, selective functionalization of the end groups in the dendrimer, leading to Janus dendrimers, may be used to control their interfacial stability. Shown in Figure 5 are the free energy profiles for the uniform dendrimer (in poor solvent) and the Janus dendrimers (again due to the symmetry of the molecules these profiles are symmetric about z=0). In all cases, due to the amphiphilic nature of the molecules, the Janus dendrimers are more stable at the interface than the uniform dendrimer (similar to amphiphilic nanoparticles [20]and proteins[19]). For the Janus dendrimers there are, however, significant differences between the different configurations investigated here. The dendrimer with separated end groups (Figure 1(b)) is the most stable, while the alternating configuration (Figure 1(c)) is the least, suggesting that spatially segregating the different end group types leads to high stability. This is in agreement with recent atomistic simulations performed on silica nanoparticles, in which it was found that nanoparticles with randomly distributed (hydrophobic) methyl groups have lower detachment energies than Janus particles with methyl groups on one face of the particle.[32] The free energy profile for the randomly functionalized dendrimer (Figure 5d) lies between the separated and alternating dendrimers.

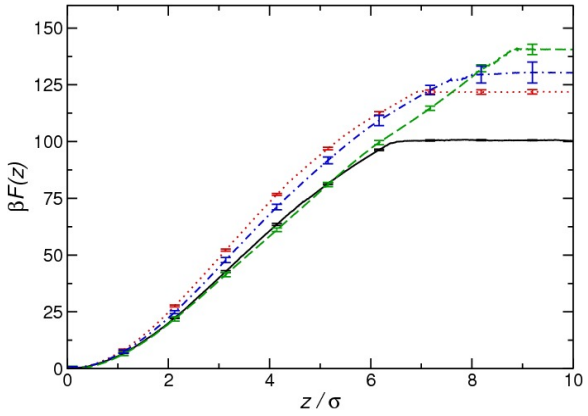

Figure 5 Free energy profile for uniform (solid line, black) in poor solvent, and Janus dendrimers with alternating (dotted line, red), random (dot-dashed line, blue) and separated (dashed line, green), end groups.

The range of the dendrimer-interface interaction also depends on the dendrimer configuration, with the separated dendrimer having the longest interaction range and the alternating the shortest. Due to the difference in the placement of the end groups the dendrimers conformational behaviour at the interface is altered. It is interesting to notice here that simulations performed on the hard-sphere model do not predict any changes in the interfacial energy range as a function of the fraction of surface area favouring one solvent over the other [20] as they do not take into account the possible change in the molecule global configuration. As shown in Figure 6(a) the profile of the radius of gyration of the Janus dendrimers is similar to the uniform case, with a peak at the interface and

another further out. However, the position and height of the second peak change as a function of the distribution of the end-groups among the dendrons, with the separated dendrimer having a larger peak further from the interface. This is clearly related to the placement of the different end groups on the dendrimer surface: due to the segregation of the two different types of end groups on its surface, the dendrimer can stretch into the solvent phase moving away from the interface while keeping the E1 (E2) beads in contact with the S1 (S2) solvent. This may be seen from simulation snapshots (Figure 6(b)) which show the differences in conformation for the different dendrimer configurations. In particular for the separated dendrimer, a dendron consisting of purely E1 beads is able to remain in contact with the S1 solvent (its favoured solvent) to large dendrimer-interface separations, stretching to the maximum its flexible structure. Such a conformation is less favourable for the alternating dendrimer as only two E1 (E2) beads can remain in contact with the interface as it moves deeper into the S1 (S2) solvent. Such type of ability of the dendrimer structure to modify its configuration to maximize favourable interactions has been also observed in atomistic simulations of alkyl-modified polyamino amide dendrimers at air/water interface. [23]

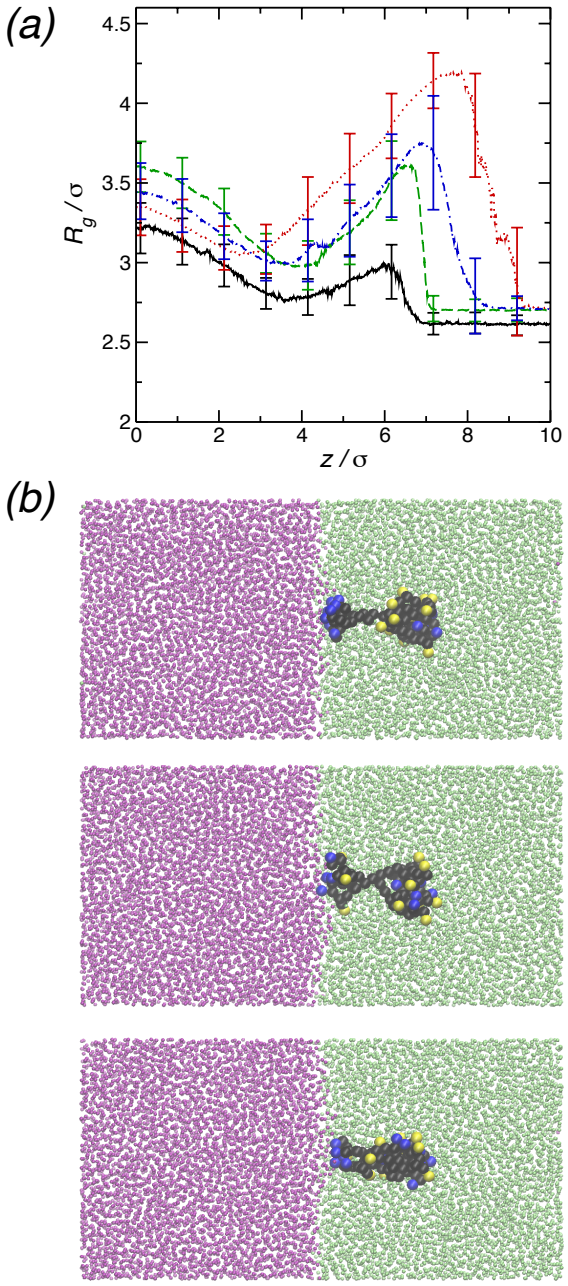

Figure 6(a) Radii of gyration for uniform (solid line, black), and Janus dendrimers with alternating (dotted line, red), separated (dashed line, green), and random (dot-dashed line, blue) end groups. (b) Simulation snapshots of Janus dendrimers near liquid-liquid interface. Top panel shows separated dendrimer with z=8σ, middle panel shows alternated dendrimer with z=6 σ, and bottom panel shows random dendrimer with z=7 σ. Beads coloured as in Figure 3(a).

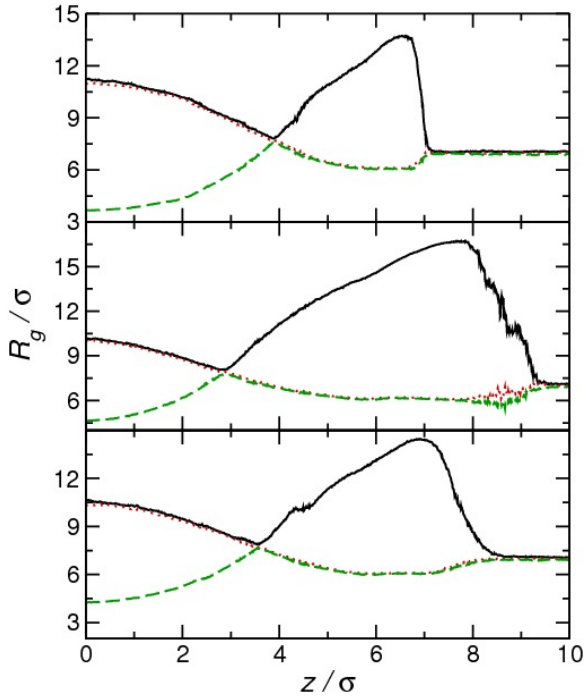

Figure 7. Axis lengths (λ_{max} (black, solid line), λ_{mid} (red, dotted line), and λ_{min} (green, dashed line)) for Janus dendrimers with alternating (top), separated (middle), and random (bottom) end groups.

The Janus dendrimers undergo similar shape changes as the uniform dendrimer, going from spherical in bulk solvent to disk-like at the interface via a rod-like structure at intermediate separations. At the interface the alternating dendrimer adopts the most disk-like shape, allowing the E1 and E2 beads of the same dendron to be in the S1 and S2 solvents respectively. Further from the interface the separated dendrimeris the most rod-like, as the purely E1 (E2) dendron remains in contact with the S1 (S2) solvent. The separations at which the dendrimer changes from disk to rod to spherical depends on the dendrimer configuration, with the alternating dendrimer having the widest region of disk-like conformation, whereas the separated dendrimer has the widest rod-like region. In the rod-like region λ_{min} and λ_{mid} are approximately equal for all the dendrimer configurations.

More information on the structure of the dendrimer may be obtained by studying the angular distribution of the end groups (with respect to the dendrimer centre of mass). Specifically the angle θ between the (unit) vector joining each end bead and the dendrimer centre of mass and the z-axis (interface normal) reveals whether the end group is pointing toward the S1 ($\cos\theta<0$) or S2 ($\cos\theta>0$) solvents, as illustrated in Figure 8(a). Shown in Figure 8(b) is the average value of $\cos\theta$ as a function of dendrimer z-coordinate for the three Janus dendrimer models. Clearly dendrimers where the different end monomers, E1 and E2, are segregated within separated dendrons (red lines in Figure 8) are more efficient in keeping their peripheral monomers in contact with the interface and therefore in contact with the favoured solvent maximizing in this way their free energy of desorption.

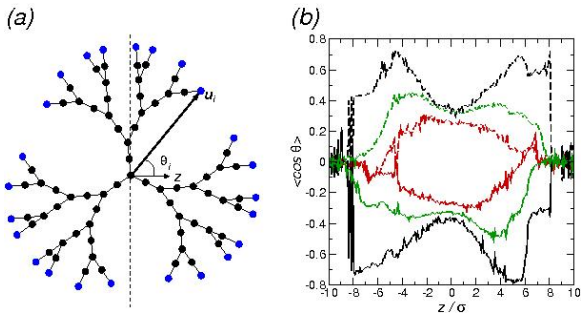

Figure 8 (a) Schematic illustration of θ (b) Average value of cos θ (see text) against dendrimer z position for seperate (black), alternating (red), and random (green) Janus dendrimers. Solid lines denote averages for E1 beads, dashed line E2 beads.

Effect of Dendrimer rigidity

Experimentally different rigidity can be imparted to the dendrimer scaffold by choosing specific monomers during the synthesis. [33] As expected, the behaviour, and therefore applications, of rigid dendrimers such as polyphenylene ones is quite different compared with the flexible ones. [34] They for example do not show any backfolding of the arms (usually seen in all flexbile dendrimers) [35] leaving the central core of the molecules sterically accessible[36, 37]and present a lower bulk density compared to the flexible one. [24] The interfacial properties of rigid dendrimers are also quite different than those of the flexible ones. When a rigid dendrimer is at the interface separating two solvents with which it interacts unfavourably, the free energy of desorption increases to 150 k_BT compared with 100 k_BT obtained for the flexible dendrimer in a similar configuration (see Figure 9). This increase in free energy is due to the fact that the dendrimer structure cannot collapse to avoid the contact with the solvent molecules when is placed in the bulk phase. The increase in stability may also be due to the increase in the interfacial area occupied by the rigid dendrimer (A=109 σ^2) compared to the flexibile case (A=71 σ^2). As it can be inferred from the R_g profile reported in Figure 9 (bottom), the rigid dendrimer keeps in fact a more "open" configuration showing a R_g consistently higher than that of the flexible dendrimer.

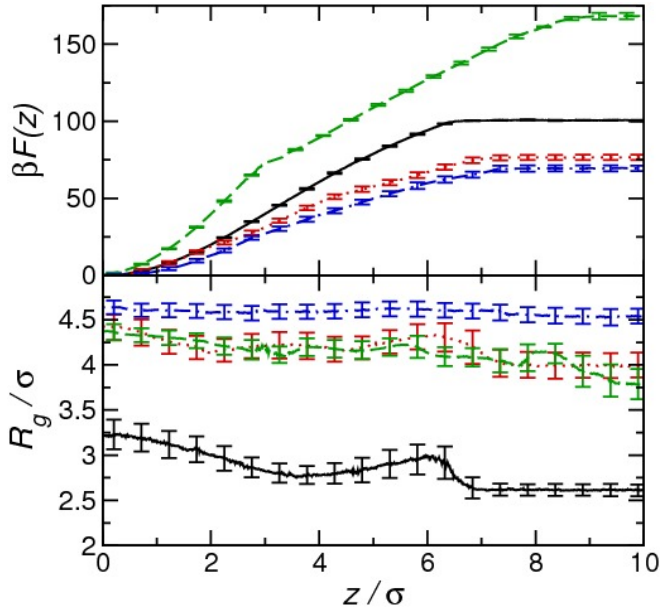

Figure 9(Top) Free energy profiles for uniform dendrimer without (solid black line, poor solvent, and dotted red line, good solvent) and with (dashed green line, poor solvent, and dot-dashed blue line, good solvent) angular potentials. (Bottom) Radius of gyration for uniform dendrimer without and with angular potentials. Colour scheme as used in the top plot.

On the contrary, when the rigid dendrimer is placed at the interface between two "good" solvents the free energy profile obtained for the rigid and flexible dendrimer models is very similar since the

conformation of the two dendrimer models (flexible and rigid one), which try to maximize the contact with both solvents, is the almost same (see also the R_g profiles of Figure 9).

Summary and Conclusions

In this paper molecular dynamics simulations are used to study the stability of model dendrimers at liquid-liquid interface. The free energy of desorption from the interface is calculated for a third generation dendrimer whose monomers are characterized by different affinity with the solvent particles. The simulation results are analysed focussing on the relationship between dendrimer functionalization (i.e. number and positions of monomers with different chemical affinity), structural flexibility and conformation.

It is found that in all cases investigated the dendrimer is stable at the interface and moves onto the solvent bulk overcoming a desorption energy barrier whose strength varies as a function of the solvent quality and dendrimer structure.

In the case of uniform dendrimer the desorption energy depends critically on solvent quality. In poor solvent the dendrimer behaviour is similar to that found for rigid nanoparticles [20] and the desorption energy is around 100 k_BT. On the contrary, in good solvent, due to the increase in number of dendrimer-solvent (favourable) interaction and the lower solvent density at the interface, the free energy barrier is quite lower (75 k_BT) and the simplified rigid model overestimates it of around 50 k_BT. The reason for this overestimation is that upon interfacial adsorption the flexible structure of the dendrimer undergoes considerable changes in shape which are neglected by the hard-sphere model; in bulk solution the dendrimer is approximately spherical, while at the interface it adopts an oblate, disk-like shape, maximising the decrease in interfacial area between the two solvent components. At intermediate separations the dendrimer adopts a rod-like shape. On the contrary, in poor solvent the dendrimer structure collapses into a spherical almost impenetrable object which behaves as a rigid nanoparticle.

The effect of distribution of monomers with different chemical affinities within the dendrimer structure is also investigated, focusing on two canonical examples. The first model tested is the so-called core-shell structure where the interior and exterior monomers have affinities for different solvent components. This uneven distribution of monomer among the dendrimer structure greatly increases the interfacial stability of the macromolecule at the interface, mainly due to the maximisation of the favourable contacts between the dendrimer monomers and solvent particles.

It is found that the energetic barrier for entry into the favoured solvent for the only dendrimer interior monomers is quite small compared with that to enter into the solvent favoured only by the external ones; this is due to the dendrimer's relatively open structure that allows solvent to

penetrate into the interior and the fact that there are many more monomers in the dendrimer interior than on its surface (67 against 24). More interestingly if compared with the energy barrier of adsorption calculated for the uniform dendrimer in poor solvent (100 k_BT), the increased stability of the core-shell one (250 k_BT) is remarkable considering also that the outer monomers are just around one third of the all number of monomers.

The effect of selectively functionalizing the dendrimer surface (so called Janus dendrimers) is also examined. This model modification also increased the interfacial stability compared to the uniform case, although the increase in stability is smaller than for the core-shell dendrimer. This result is in agreement with recent atomistic simulations of PAMAM dendrimers at the air-water interface [23] indicating that dendrimers that were fully functionalized by hydrophobic end groups were more stable than a half-functionalized Janus dendrimer. It is also found that while the magnitude of the stability depends on the precise placement of end groups on the dendrimer in all the arrangements of end groups the Janus dendrimers are more stable than the uniform case.

By including angular potentials the effect of structure rigidity on interfacial stability was also studied. When the dendrimer is at the interface between two poor-solvents the rigid dendrimer is significantly more stable than the flexible one. This increase in stability is arises as the rigid dendrimer cannot collapse in bulk solution and from the larger decrease in interfacial when the rigid dendrimer absorbs. For a dendrimer at the interface between two good-solvent the rigid dendrimer is slightly less stable.

While the work in this paper was performed on a relatively simple model, the changes to the dendrimer structure are largely realizable synthetically. Thus it should provide general guidelines for the modification of dendrimer interfacial adsorption. Future work will extend this to the study of chemically detailed models, giving the direct insight into the interfacial behaviour of experimental systems and to the study the effect of macromolecular topology on interfacial adsorption.

References

1. D. Astruc, E. Boisselier and C. Ornelas, *Chem. Rev.*, 2010, **110**, 1857-1959.
2. D. A. Tomalia, *Progress in Polymer Science*, 2005, **30**, 294-324.
3. D. A. Tomalia and J. M. Frechet, *Progress in Polymer Science*, 2005, **30**, 217-219.
4. D. C. Tully and J. M. J. Frechet, *Chemical Communications*, 2001, 1229-1239.
5. K. W. Chooi, A. I. Gray, L. Tetley, Y. L. Fan and I. F. Uchegbu, *Langmuir*, 2010, **26**, 2301-2316.
6. R. Esfand and D. A. Tomalia, *Drug Discovery Today*, 2001, **6**, 427-436.
7. J. M. J. Frechet, *Proceedings of the National Academy of Sciences of the United States of America*, 2002, **99**, 4782-4787.
8. A. Gomez-Escudero, M. A. Azagarsamy, N. Theddu, R. W. Vachet and S. Thayumanavan, *Journal of the American Chemical Society*, 2008, **130**, 11156-11163.
9. B. M. Rosen, C. J. Wilson, D. A. Wilson, M. Peterca, M. R. Imam and V. Percec, *Chem. Rev.*, 2009, **109**, 6275-6540.
10. A. Schenning, C. Elissen-Roman, J. W. Weener, M. Baars, S. J. van der Gaast and E. W. Meijer, *Journal of the American Chemical Society*, 1998, **120**, 8199-8208.
11. G. Sui, M. Mabrouki, Y. Ma, M. Micic and R. M. Leblanc, *Journal of Colloid and Interface Science*, 2002, **250**, 364-370.
12. V. Percec, D. A. Wilson, P. Leowanawat, C. J. Wilson, A. D. Hughes, M. S. Kaucher, D. A. Hammer, D. H. Levine, A. J. Kim, F. S. Bates, K. P. Davis, T. P. Lodge, M. L. Klein, R. H. DeVane, E. Aqad, B. M. Rosen, A. O. Argintaru, M. J. Sienkowska, K. Rissanen, S. Nummelin and J. Ropponen, *Science*, 2010, **328**, 1009-1014.
13. A. M. Caminade, R. Laurent, B. Delavaux-Nicot and J. P. Majoral, *New J. Chem.*, 2012, **36**, 217-226.
14. P. Pieranski, *Phys. Rev. Lett.*, 1980, **45**, 569-572.
15. R. Aveyard, B. D. Beake and J. H. Clint, *J. Chem. Soc.-Faraday Trans.*, 1996, **92**, 4271-4277.
16. F. Bresme and M. Oettel, *J. Phys.-Condes. Matter*, 2007, **19**, 413101-413134.
17. D. L. Cheung and S. A. F. Bon, *Phys. Rev. Lett.*, 2009, **102**, 066103-066107.
18. D. L. Cheung, *J. Chem. Phys.*, 2011, **135**, 8.
19. D. L. Cheung, *Langmuir : the ACS journal of surfaces and colloids*, 2012, **28**, 8730-8736.
20. D. L. Cheung and S. A. F. Bon, *Soft Matter*, 2009, **5**, 3969-3976.
21. H. Lehle and M. Oettel, *J. Phys.-Condes. Matter*, 2008, **20**, 10.
22. K. A. Tay and F. Bresme, *Journal of the American Chemical Society*, 2006, **128**, 14166-14175.
23. S. Nawaz and P. Carbone, *J. Phys. Chem. B*, 2011, **115**, 12019-12027.
24. P. Carbone and L. Lue, *Macromolecules*, 2010, **43**, 9191-9197.
25. G. M. Torrie and J. P. Valleau, *J. Comput. Phys.*, 1977, **23**, 187-199.
26. S. Kumar, D. Bouzida, R. H. Swendsen, P. A. Kollman and J. M. Rosenberg, *J. Comput. Chem.*, 1992, **13**, 1011-1021.
27. S. Plimpton, *J. Comput. Phys.*, 1995, **117**, 1-19.
28. G. J. Martyna, D. J. Tobias and M. L. Klein, *J. Chem. Phys.*, 1994, **101**, 4177-4189.
29. K. Du, E. Glogowski, T. Emrick, T. P. Russell and A. D. Dinsmore, *Langmuir*, 2010, **26**, 12518-12522.
30. J. J. Muller and H. Schrauber, *J. Appl. Crystallogr.*, 1992, **25**, 181-191.
31. R. Ranatunga, R. J. B. Kalescky, C. C. Chiu and S. O. Nielsen, *J. Phys. Chem. C*, 2010, **114**, 12151-12157.
32. H. Fan, D. E. Resasco and A. Striolo, *Langmuir*, 2011, **27**, 5264-5274.
33. A. J. Berresheim, M. Muller and K. Mullen, *Chem. Rev.*, 1999, **99**, 1747-1785.
34. M. Schlupp, T. Weil, A. J. Berresheim, U. M. Wiesler, J. Bargon and K. Müllen, *Angew. Chem.-Int. Edit.*, 2001, **40**, 4011.
35. P. Carbone and F. Müller-Plathe, *Soft Matter*, 2009, **5**, 2638-2647.
36. P. Carbone, A. Calabretta, M. Di Stefano, F. Negri and K. Müllen, *Journal of Physical Chemistry A*, 2006, **110**, 2214-2224.
37. P. Carbone, F. Negri and F. Müller-Plathe, *Macromolecules*, 2007, **40**, 7044-7055.